Supernova Ia and Galaxy Cluster Gas Mass Fraction Constraints on Dark Energy

Kyle M. Wilson, Gang Chen,[1] and Bharat Ratra

Department of Physics, Kansas State University, 116 Cardwell Hall, Manhattan, KS 66506; kmwilson, chengang, ratra@phys.ksu.edu

ABSTRACT

We use the Riess et al. (2004) supernova Ia apparent magnitude versus redshift data and the Allen et al. (2004) galaxy cluster gas mass fraction versus redshift data to constrain dark energy models. These data provide complementary constraints that when combined together significantly restrict model parameters and favor slowly-evolving dark energy density models, close to the Einstein cosmological constant limit of dark energy.

Subject headings: cosmology: cosmological parameters—cosmology: observations—X-rays: galaxies: clusters—supernovae: general

1.   Introduction

Less than a decade ago, astronomers discovered that the expansion of the Universe was speeding up (Riess et al. 1998; Perlmutter et al. 1999). In the context of Einstein's general relativity, this acceleration is attributed to dark energy that varies slowly with time and space, if at all. More recent supernova Ia (SNIa) redshift-magnitude data,[2] and cosmic microwave background (CMB) anisotropy data — that indicates the Universe is spatially

---

[1]Present address: Institute for Astronomy, 2680 Woodlawn Drive, Honolulu, HI 96822; gchen@ifa.hawaii.edu

[2]For the SNIa data see, e.g., Riess et al. (2004, hereafter R04), Nobili et al. (2005), Clocchiatti et al. (2006), and Astier et al. (2006). SNIa data constraints on cosmological parameters are also discussed by Wang & Tegmark (2005), Lazkoz et al. (2005), Hannestad (2005), Shafieloo et al. (2006), Zhang & Wu (2005), Godłowski & Szydłowski (2005), Sethi et al. (2005), Bento et al. (2005), and Jassal et al. (2006).

flat (see, e.g., Podariu et al. 2001b; Durrer et al. 2003; Melchiorri & Ödman 2003; Bennett et al. 2003; Page et al. 2003) — combined with a low mean value for the nonrelativistic matter density parameter Ω_M (Chen & Ratra 2003b, and references therein), strengthens the claim that a previously undetected dark energy accounts for a major part of the cosmic energy budget. For reviews of the current situation see Peebles & Ratra (2003), Steinhardt (2003), Carroll (2004), Padmanabhan (2005), and Perivolaropoulos (2006).

While CMB anisotropy and SNIa constraints on dark energy will continue to improve,[3] it is important to use many different tests to constrain dark energy models. This will allow for consistency checks, as well as provide complementary constraints on dark energy. A number of other tests have been considered. These include the redshift-angular size test (see, e.g., Chen & Ratra 2003a; Podariu et al. 2003; Jackson 2004; Puetzfeld et al. 2005; Daly & Djorgovski 2005), the strong gravitational lensing test (see, e.g., Fukugita et al. 1990; Turner 1990; Ratra & Quillen 1992; Chae et al. 2004; Sereno 2005; Alcaniz et al. 2005), the galaxy cluster gas mass fraction versus redshift test (see, e.g., Sasaki 1996; Pen 1997; Allen et al. 2004, hereafter A04; Chen & Ratra 2004, hereafter CR; Rapetti et al. 2005; Alcaniz & Zhu 2005; Kravtsov et al. 2005; Chang et al. 2006), and the baryon acoustic oscillation test (see, e.g., Glazebrook & Blake 2005; Angulo et al. 2005; Wang 2006). In addition, structure formation in dark energy models will soon provide a useful diagnostic of model parameters (see, e.g., Horellou & Berge 2005; McDonald et al. 2006; Le Delliou 2005; Bartelmann et al. 2005; Percival 2005; Mainini 2005). In this paper we constrain dark energy models by doing a joint analysis of the SNIa apparent magnitude versus redshift data of R04 and the galaxy cluster gas mass fraction versus redshift data of A04.

There are a number of different dark energy models under current discussion.[4] The current "standard" cosmological model is ΛCDM (Peebles 1984), where the energy density of the low-redshift Universe is dominated by a cosmological constant Λ (with a constant energy density ρ_Λ), with nonrelativistic matter — mostly cold dark matter (CDM) — playing a subdominant role. Models in which the dark energy is due to a slowly varying, in time and space, scalar field (ϕ), have also attracted recent attention. A prototypical ϕCDM example

---

[3]For near future SNIa constraints see Sollerman et al. (2005) and Hamuy et al. (2006). Within a decade or so, the proposed JDEM/SNAP space mission should provide even tighter constraints (see http://snap.lbl.gov/ and Podariu et al. 2001a; Crotts et al. 2005; Albert et al. 2005, and references therein). Mukherjee et al. (2003), Caldwell & Doran (2004), and Lee et al. (2006) discuss CMB constraints on dark energy.

[4]Recent papers include Neupane & Wiltshire (2005), Pietroni (2005), Zhao et al. (2005), Capozziello et al. (2005), França (2005), Barenboim et al. (2005), Barnes et al. (2005), Abdel-Rahman & Riad (2005), Barger et al. (2005), Solá & Štefančić (2006), and Arbey (2006).

has scalar field potential energy density $V(\phi) \propto \phi^{-\alpha}, \alpha > 0$, at low redshift (Peebles & Ratra 1988; Ratra & Peebles 1988); again CDM plays a subdominant role. Also discussed is the XCDM parametrization for time-varying dark energy. This parametrization approximates dark energy by a fluid with a negative time-independent equation of state parameter $w = P/\rho$, where P is the fluid pressure and ρ the energy density. This is an inaccurate approximation during the scalar field dominated epoch when w is time dependent (see, e.g., Ratra 1991). We consider spatially flat spacetimes for the ϕCDM model and the XCDM parametrization, but allow spatial curvature to be a free parameter in the ΛCDM case. In this paper we constrain parameters of these three models by using SNIa and galaxy cluster data.

In § 2 we show how we use the supernova and galaxy cluster data to constrain cosmological parameters. Results are presented and discussed in § 3. We conclude in § 4.

2. Computation

A04 list x-ray gas mass fractions for 26 rich clusters, determined from *Chandra* observations. These clusters lie at redshifts between 0.08 and 0.89. Following A04 and CR, we use this data to determine the probability distribution function (likelihood) $L^G(\Omega_M, p, h)$. Here h is the Hubble constant in units of $100 \ \mathrm{km \, s^{-1} Mpc^{-1}}$, and p is the cosmological constant density parameter Ω_Λ for the ΛCDM model, w for the XCDM parametrization, and α for the ϕCDM model. To derive $L^G(\Omega_M, p, h)$ we marginalize over the bias factor b, as well as over $\Omega_b h^2$, where Ω_b is the baryonic mass density parameter. Later we will need to marginalize over h. We account for uncertainties in b, $\Omega_b h^2$, and h by using Gaussian priors with $b = 0.824 \pm 0.089$, $\Omega_b h^2 = 0.0214 \pm 0.002$, and $h = 0.72 \pm 0.08$, all one standard deviation errors.[5] See A04 and CR for more detailed discussions of the procedure we use.

We also use the SNIa apparent magnitude versus redshift data from R04, in particular, the gold data set of 156 SNIa with redshifts up to almost 1.8. From this data we determine

---

[5]See Ganga et al. (1997) for a discussion of this method. As noted in CR, there is a more precise estimate of h than the value quoted above, $h = 0.68 \pm 0.04$ (Gott et al. 2001; Chen et al. 2003, and we have halved the quoted two standard deviation errors). Also, the $\Omega_b h^2$ value used above is consistent with the estimate from the WMAP CMB anisotropy measurement and the primordial deuterium abundance measurement, but significantly higher than an estimate based on the primordial helium and lithium abundance measurements (see, e.g., Peebles & Ratra 2003; Steigman 2005; Fields & Sarkar 2006), so we also consider the Peebles & Ratra (2003) summary estimate $\Omega_b h^2 = 0.014 \pm 0.004$. Constraints derived using the values of h and $\Omega_b h^2$ quoted in this footnote are shown as darker dashed lines in Figs. 2—4, while constraints from the priors quoted in the main text are shown using lighter continuous lines.

the probability distribution function $L^S(\Omega_M, p, h)$, following, e.g., R04 or Podariu & Ratra (2000).

The joint likelihood for the SNIa and galaxy cluster data is the product of the two individual likelihoods. The two-dimensional probability distribution function for Ω_M and p, $L(\Omega_M, p)$, is determined by marginalizing this product over h. For each of the three models mentioned above, we compute $L(\Omega_M, p)$ on the two-dimensional (Ω_M, p) grid. The 1, 2, and 3 σ confidence contours are the set of points where the likelihood is $e^{-2.30/2}$, $e^{-6.17/2}$, and $e^{-11.8/2}$ of the maximum likelihood value.

3. Results and Discussion

Figure 1 shows the R04 gold SNIa constraints on the ϕCDM model with $V(\phi) \propto \phi^{-\alpha}$, determined by marginalizing $L^S(\Omega_M, \alpha, h)$ over h. These contours are significantly more constraining than those derived by Podariu & Ratra (2000, Fig. 1) from earlier SNIa data.

Figure 2 shows the combined SNIa and galaxy cluster constraints on the ΛCDM model. These joint constraints are significantly tighter than those derived using either the SNIa data (R04, Fig. 8) or the galaxy cluster data (A04, Figs. 4 and 8; CR, Fig. 1) alone. This is because the galaxy cluster data tend to tightly constrain Ω_M (A04, CR), while the SNIa data tend to tightly constrain a linear combination of Ω_Λ and Ω_M (R04). Together, the data focus attention on a small part of parameter space near $\Omega_M \sim 0.3$ and $\Omega_\Lambda \sim 0.7$ where the Universe is spatially flat.

Figure 3 shows the joint data constraints on the XCDM parametrization. Models close to $\Omega_M \sim 0.3$ and $w \sim -1$ are favored. We emphasize that $w = -1$ corresponds to the spatially-flat ΛCDM model.

Figure 4 shows the joint data constraints on the ϕCDM model with $V(\phi) \propto \phi^{-\alpha}$. Models close to $\Omega_M \sim 0.25$ and $\alpha \sim 0$ are favored. We note that $\alpha = 0$ corresponds to the spatially-flat ΛCDM model.

The SNIa and galaxy cluster data together favor a spatially-flat ΛCDM model with $\Omega_M \approx 0.25 - 0.3$. It might be significant that other data also favor this value of Ω_M (see, e.g., Chen & Ratra 2003b; Spergel et al. 2003). We emphasize, however, that slowly-evolving dark energy models are also consistent with this data.

4. Conclusion

We use supernova Ia apparent magnitude and x-ray cluster gas mass fraction data to jointly constrain cosmological parameters. These data sets provide complementary constraints and together they tightly constrain cosmological parameters. The spatially-flat ΛCDM model is favored, although a ϕCDM model with slowly-decreasing dark energy cannot yet be ruled out.

More and better SNIa and galaxy cluster data will allow for tighter constraints on model parameters. Equally important would be a resolution of the conflict between the two different sets of estimates of Ω_b, as well as tighter limits on h. All these are likely to happen in the next few years.

REFERENCES

Abdel-Rahman, A.-M. M., & Riad, I. F. 2005, astro-ph/0512612

Albert, J., et al. 2005, astro-ph/0507458

Alcaniz, J. S., Dev, A., & Jain, D. 2005, ApJ, 627, 26

Alcaniz, J. S., & Zhu, Z.-H. 2005, Phys. Rev. D, 71, 083513

Allen, S. W., Schmidt, R. W., Ebeling, H., Fabian, A. C., & van Speybroeck, L. 2004, MNRAS, 353, 457 (A04)

Angulo, R., et al. 2005, MNRAS, 362, L25

Arbey, A. 2006, astro-ph/0601274

Astier, P., et al. 2006, A&A, 447, 31

Barenboim, G., Requejo, O. M., & Quigg, C. 2005, astro-ph/0510178

Barger, V., Guarnaccia, E., & Marfatia, D. 2005, hep-ph/0512320

Barnes, L., Francis, M. J., Lewis, G. F., & Linder, E. V. 2005, astro-ph/0510791

Bartelmann, M., Doran, M., & Wetterich, C. 2005, astro-ph/0507257

Bennett, C. L., et al. 2003, ApJS, 148, 1

Bento, M. C., Bertolami, O., Santos, N. M. C., & Sen, A. A. 2005, astro-ph/0512076

Caldwell, R., & Doran, M. 2004, Phys. Rev. D, 69, 103517

Capozziello, S., Cardone, V. F., Elizalde, E., Nojiri, S., & Odintsov, S. D. 2005, astro-ph/0508350

Carroll, S. M. 2004, in Measuring and Modeling the Universe, ed. W. L. Freedman (Cambridge:Cambridge University Press), 235

Chae, K.-H., Chen, G., Ratra, B., & Lee, D.-W. 2004, ApJ, 607, L71

Chang, Z., Wu, F.-Q., & Zhang, X. 2006, Phys. Lett. B, 633, 14

Chen, G., Gott, J. R., & Ratra, B. 2003, PASP, 115, 1269

Chen, G., & Ratra, B. 2003a, ApJ, 582, 586

Chen, G., & Ratra, B. 2003b, PASP, 115, 1143

Chen, G., & Ratra, B. 2004, ApJ, 612, L1 (CR)

Clocchiatti, A., et al. 2006, ApJ, 627, (astro-ph/0510155)

Crotts, A., et al. 2005, astro-ph/0507043

Daly, R. A., & Djorgovski, S. G. 2005, astro-ph/0512576

Durrer, R., Novosyadlyj, B., & Apunevych, S. 2003, ApJ, 583, 33

Fields, D., & Sarkar, S. 2006, astro-ph/0601514

França, U. 2005, astro-ph/0509177

Fukugita, M., Futamase, T., & Kasai, M. 1990, MNRAS, 241, 24P

Ganga, K., Ratra, B., Gundersen, J. O., & Sugiyama, N. 1997, ApJ, 484, 7

Glazebrook, R., & Blake, C. 2005, ApJ, 631, 1

Godłowski, W., & Szydłowski, M. 2005, Phys. Lett. B, 623, 10

Gott, J. R., Vogeley, M. S., Podariu, S., & Ratra, B. 2001, ApJ, 549, 1

Hamuy, M., et al. 2006, PASP, 118, 2

Hannestad, S. 2005, Phys. Rev. D, 71, 103519

Horellou, C., & Berge, J. 2005, MNRAS, 360, 1393

Jackson, J. C. 2004, J. Cosmo. Astropart. Phys., 11, 007

Jassal, H. K., Bagla, J. S., & Padmanabhan, T. 2006, astro-ph/0601389

Kravtsov, A. V., Nagai, D., & Vikhlinin, A. A. 2005, ApJ, 625, 588

Lazkoz, R., Nesseris, S., & Perivolaropoulos, L. 2005, J. Cosmo. Astropart. Phys., 11, 10

Le Delliou, M. 2005, astro-ph/0506200

Lee, S., Liu, G.-C., & Ng, K.-W. 2006, astro-ph/0601333

Mainini, A. 2005, Phys. Rev. D, 72, 083514

McDonald, P., Trac, H., & Contaldi, C. 2006, MNRAS, 366, 547

Melchiorri, A., & Ödman, C. J. 2003, Phys. Rev. D, 67, 081302

Mukherjee, P., Banday, A. J., Riazuelo, A., Górski, K. M., & Ratra, B. 2003, ApJ, 598, 767

Neupane, I. P., & Wiltshire, D. L. 2005, Phys. Rev. D, 72, 083509

Nobili, S., et al. 2005, A&A, 437, 789

Padmanabhan, T. 2005, Curr. Sci. 88, 1057

Page, L., et al. 2003, ApJS, 148, 233

Peebles, P. J. E. 1984, ApJ, 284, 439

Peebles, P. J. E., & Ratra, B. 1988, ApJ, 325, L17

Peebles, P. J. E., & Ratra, B. 2003, Rev. Mod. Phys., 75, 559

Pen, U. 1997, New Astron., 2, 309

Percival, W. J. 2005, A&A, 443, 819

Perivolaropoulos, L. 2006, astro-ph/0601014

Perlmutter, S., et al. 1999, ApJ, 517, 565

Pietroni, M. 2005, Phys. Rev. D, 72, 043535

Podariu, S., Daly, R. A., Mory, M., & Ratra, B. 2003 ApJ, 584, 577

Podariu, S., Nugent, P., & Ratra, B. 2001a, ApJ, 553, 39

Podariu, S., & Ratra, B. 2000, ApJ, 532, 109

Podariu, S., Souradeep, T., Gott, J. R., Ratra, B., & Vogeley, M. S. 2001b, ApJ, 559, 9

Puetzfeld, D., Pohl, M., & Zhu, Z.-H. 2005, ApJ, 619, 657

Rapetti, D., Allen, S. W., & Weller, J. 2005, MNRAS 360, 555

Ratra, B. 1991, Phys. Rev. D, 43, 3802

Ratra, B., & Peebles, P. J. E. 1988, Phys. Rev. D, 37, 3406

Ratra, B., & Quillen, A. 1992, MNRAS, 259, 738

Riess, A. G., et al. 1998, AJ, 116, 1009

Riess, A. G., et al. 2004, ApJ, 607, 665 (R04)

Sasaki, S. 1996, PASJ, 48, L119

Sereno, M. 2005, MNRAS 356, 937

Sethi, G., Singh, S. K., Kumar, P., Jain, D., & Dev, A. 2005, astro-ph/0508491

Shafieloo, A., Alam, U., Sahni, V., & Starobinsky, A. A. 2006, MNRAS, in press (astro-ph/0505329)

Solá, J., & Štefančić, H. 2006, gr-qc/0601012

Sollerman, J., et al. 2005, astro-ph/0510026

Spergel, D. N., et al. 2003, ApJS, 148, 175

Steigman, G. 2005, Int. J. Mod. Phys. E, 15, 1

Steinhardt, P. J. 2003, Phil. Trans. Roy. Soc. Lond. A, 361, 2497

Turner, E. L. 1990, ApJ, 365, L43

Wang, Y. 2006, astro-ph/0601163

Wang, Y., & Tegmark, M. 2005, Phys. Rev. D, 71, 103513

Zhang, X., & Wu, F.-Q. 2005, Phys. Rev. D, 72, 043524

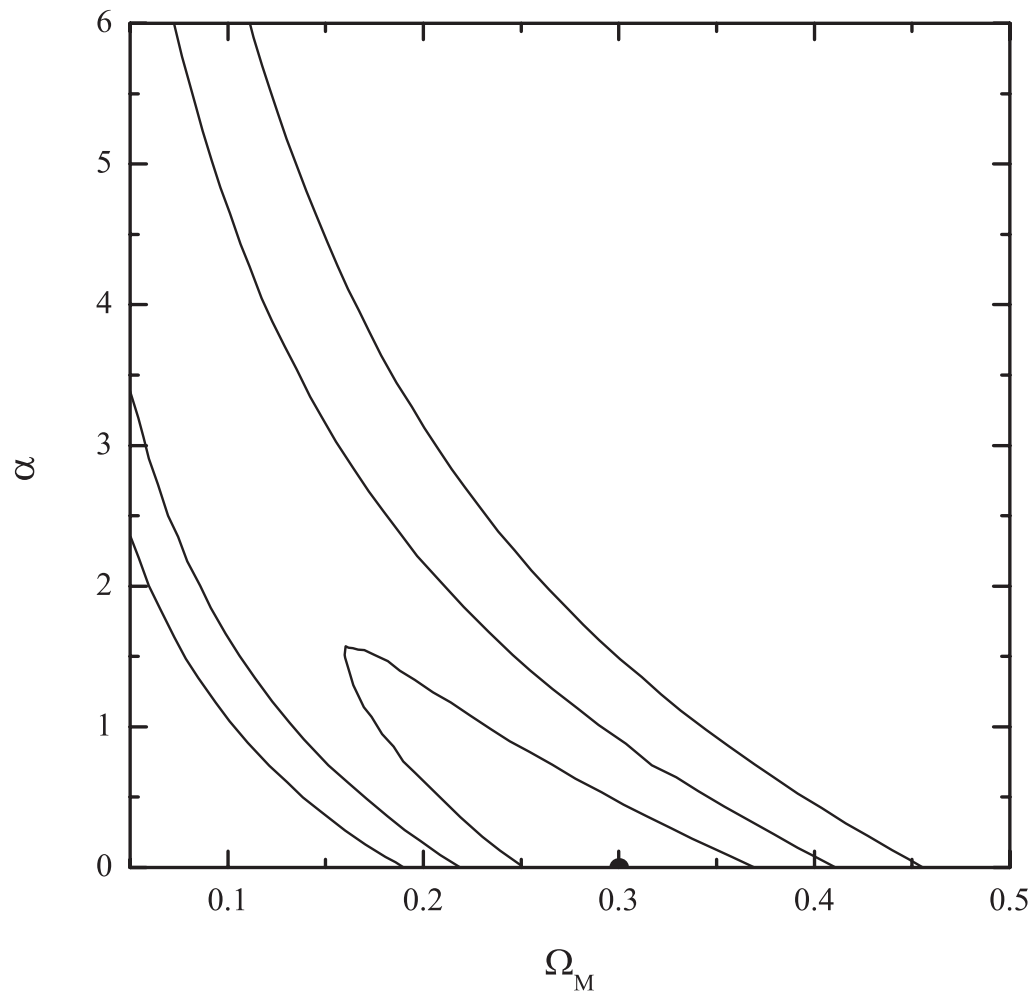Zhao, G.-B., Xia, J.-Q., Li, M., Feng, B., & Zhang, X. 2005, Phys. Rev. D, 72, 123515

Fig. 1.— Probability distribution function confidence contours (1, 2, and 3 σ from inside to outside) for the ϕCDM model using the R04 gold SNIa sample. The dot denotes the maximum likelihood and is at $\Omega_M = 0.30$ and $\alpha = 0.0$.
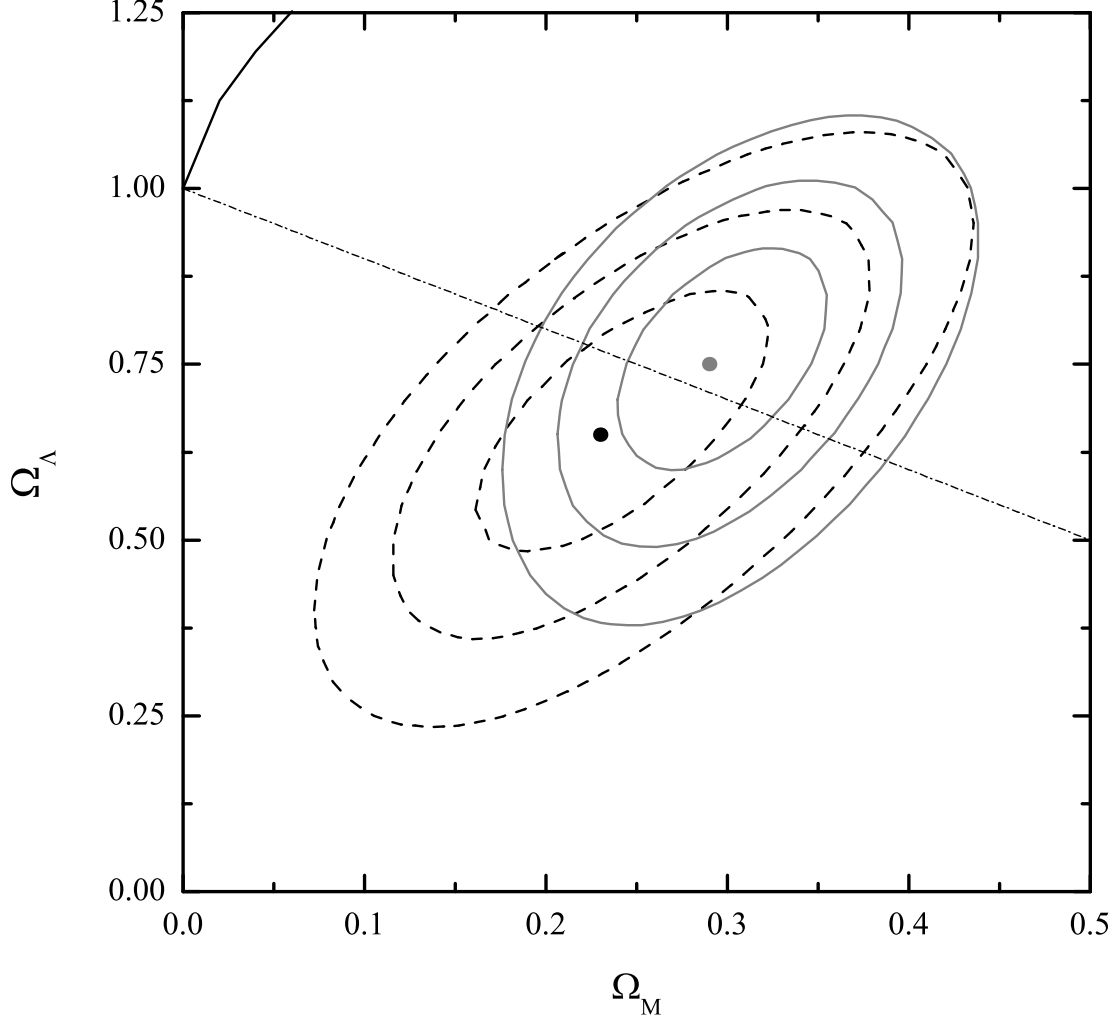
Fig. 2.— Probability distribution function confidence contours (1, 2, and 3 σ from inside to outside) for the ΛCDM model. The solid gray lines are computed using $h = 0.72 \pm 0.08$ and $\Omega_b h^2 = 0.0214 \pm 0.002$, with maximum likelihood at $\Omega_M = 0.29$ and $\Omega_\Lambda = 0.75$. The black dotted lines use $h = 0.68 \pm 0.04$ and $\Omega_b h^2 = 0.014 \pm 0.004$, with maximum likelihood at $\Omega_M = 0.23$ and $\Omega_\Lambda = 0.65$. The slanting dash-dot line indicates spatially-flat models and models to the left and above the solid black line in the left top corner do not have a big bang.
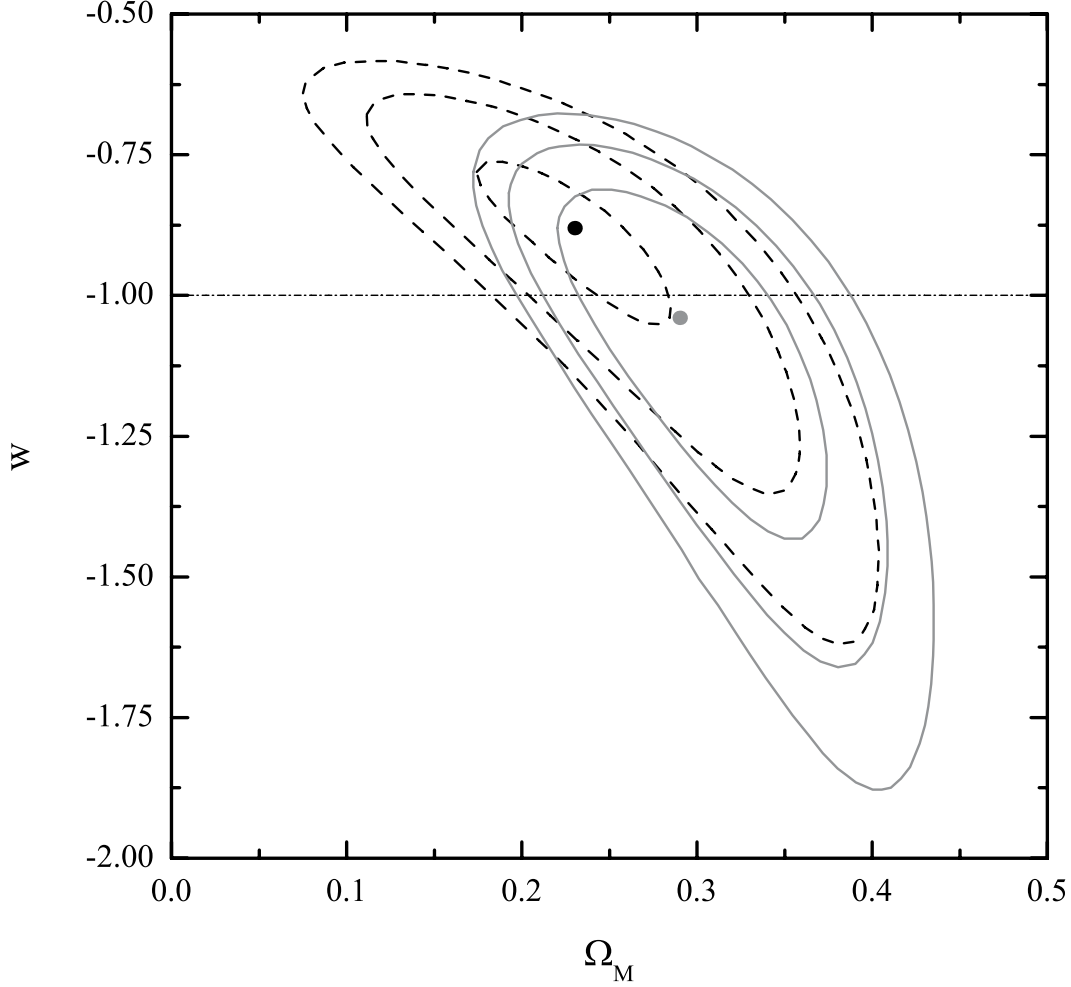
Fig. 3.— Probability distribution function confidence contours (1, 2, and 3 σ from inside to outside) for the XCDM parametrization. The solid gray lines are computed using $h = 0.72\pm0.08$ and $\Omega_b h^2 = 0.0214\pm0.002$, with maximum likelihood at $\Omega_M = 0.29$ and $w = -1.04$. The black dotted lines use $h = 0.68\pm0.04$ and $\Omega_b h^2 = 0.014\pm0.004$, with maximum likelihood at $\Omega_M = 0.23$ and $w = -0.88$. The horizontal dash-dot line at $w = -1$ indicates spatially-flat ΛCDM models.
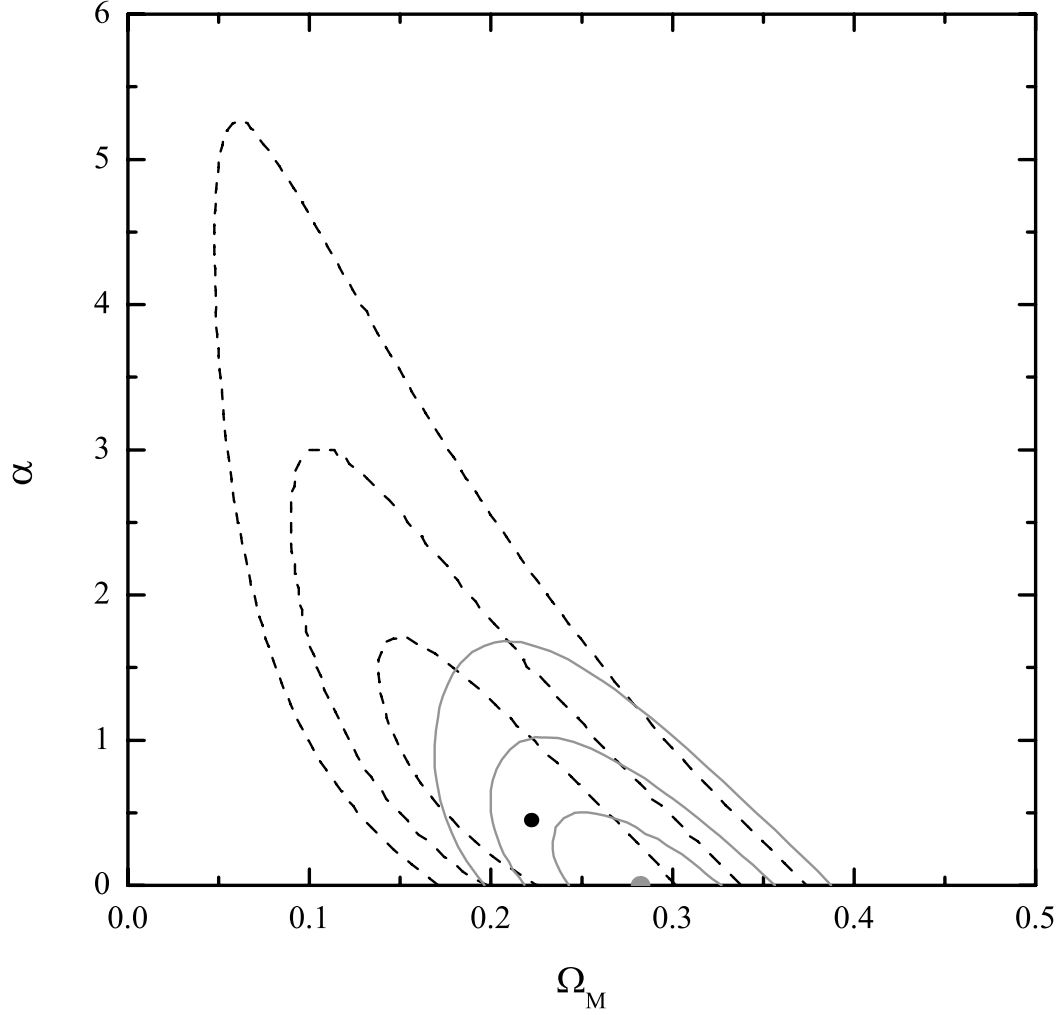
Fig. 4.— Probability distribution function confidence contours (1, 2, and 3 σ from inside to outside) for the ϕCDM model with $V(\phi) \propto \phi^{-\alpha}$. The solid gray lines are computed using $h = 0.72 \pm 0.08$ and $\Omega_b h^2 = 0.0214 \pm 0.002$, with maximum likelihood at $\Omega_M = 0.28$ and $\alpha = 0.0$. The black dotted lines use $h = 0.68 \pm 0.04$ and $\Omega_b h^2 = 0.014 \pm 0.004$, with maximum likelihood at $\Omega_M = 0.22$ and $\alpha = 0.45$. The horizontal $\alpha = 0$ axis corresponds to spatially-flat ΛCDM models.